Excited-state quantum phase transitions in the two-spin elliptic Gaudin model

Armando Relaño,[1] Carlos Esebbag,[2] and Jorge Dukelsky[3]
[1]*Departamento de Física Aplicada I and GISC, Universidad Complutense de Madrid, Avenida Complutense s/n, 28040 Madrid, Spain*
[2]*Departamento de Física y Matemáticas, Universidad de Alcalá, E-28871 Alcalá de Henares, Spain*
[3]*Instituto de Estructura de la Materia, Consejo Superior de Investigaciones Científicas, Serrano 123, E-28006 Madrid, Spain*
(Received 1 August 2016; published 4 November 2016)

We study the integrability of the two-spin elliptic Gaudin model for arbitrary values of the Hamiltonian parameters. The limit of a very large spin coupled to a small one is well described by a semiclassical approximation with just one degree of freedom. Its spectrum is divided into bands that do not overlap if certain conditions are fulfilled. In spite of the fact that there are no quantum phase transitions in each of the band heads, the bands show excited-state quantum phase transitions separating a region in which the parity symmetry is broken from another region in which time-reversal symmetry is broken. We derive analytical expressions for the critical energies in the semiclassical approximation, and confirm the results by means of exact diagonalizations for large systems.

DOI: 10.1103/PhysRevE.94.052110

I. INTRODUCTION

Excited-state quantum phase transitions (ESQPTs) have recently arisen as a subject of great interest in the study of quantum many-body systems with few degrees of freedom [1–4]. A quantum phase transition (QPT) is characterized by a nonanalytic change in the properties of the ground state (GS) of the system at a certain critical value of a control parameter [5], i.e., a parameter that controls a particular term in the Hamiltonian, like the interaction strength or the intensity of an external field. The critical point separates a symmetric phase from another phase with a broken symmetry, or in some cases two different broken symmetry phases. Analogously, an ESQPT describes a similar phenomenon but extended to the excited states in the spectrum [1,6]. It implies that the properties of certain excited states become nonanalytical at the critical value of the control parameter, or that the spectrum of a system with fixed values of all control parameters becomes singular at a certain critical energy. In general, QPTs and ESQPTs are related in the sense that an ESQPT is usually seen as the propagation of the QPT to excited states in the symmetry-broken phase.

ESQPTs have been identified in an important number of collective models, like the Lipkin-Meshkov-Glick (LMG) [7,8], the Dicke and Tavis Cummings models [9], the interacting boson model [10], the molecular vibron model [11], and in atom-molecule condensates [12]. They have also been found in other quantum models which become semiclassical in certain limits, like the kicked-top [13] or the Rabi model [14]. Experimental signatures of these transitions have been observed in molecular systems [15], superconducting microwave billiards [16], and spinor condensates [17].

Despite all these analytic and experimental results, ESQPTs suffer from some significative problems that preclude a complete understanding of the phenomenon. Among them, the most relevant is the absence of a clear order parameter (see, for example [4]). A promising alternative lays in the existence of symmetry-breaking equilibrium states at one side of the transition [18], entailing the irreversible restoration of the symmetry when the critical energy is crossed [19].

In this work, we study the integrable two-spin elliptic Gaudin model (TSEGM) [20] to shed some light on the foundations and features of ESQPTs, as well as on the properties of this recently recovered integrable model [21].

In general, ESQPTs are quantum manifestations of a classical bifuraction in phase space. They take place in the limit in which the quantum system approaches its classical counterpart. In the LMG, Dicke, vibron, and atom-molecule models the ESQPT occurs in the thermodynamical limit, $N \to \infty$, where N is the number of two-level atoms [7,9–12]. From this point of view, this phase transition is similar to thermal [22] or quantum phase transitions [5]. Notwithstanding, a large number of atoms is not required for this kind of critical phenomenon. For example, it has been recently shown that they also exist in the Rabi model, which consists of just one two-level atom interacting with a single frequency field [14]. In this case, the classical limit is reached when the ratio among the level splitting of the atom and the frequency of the field tends to infinity [23]. Under these circumstances the field can be treated classically, and therefore the model is described by means of two classical energy surfaces, each one corresponding to an eigenvalue of the remaining quantum part of the Hamiltonian, and having just one classical degree of freedom.

The TSEGM admits different semiclassical descriptions. The obvious one arises when the two spins tend to infinity, $s_1 \to \infty$ and $s_2 \to \infty$. The resulting description consists of a classical energy surface $H(\phi_1,\psi_1;\phi_2,\psi_2)$, with two classical degrees of freedom. This description is similar to the usual one for algebraic two fluid bosonic models [24]. However, as we shall see below, this limit $s_1 \to \infty$ and $s_2 \to \infty$ does not produce ESQPTs. Thus, we deal in this work with another semiclassical limit obtained when a small spin s_2 couples with a very large spin $s_1 \to \infty$. This situation is very similar to the one in which QPTs and ESQPTs appear in the Rabi model [14]: the small spin remains quantum, whereas the large is described classically. We will show below that ESQPTs appear under these circumstances. Furthermore, these transitions occur *without* the corresponding QPTs in the ground state. This result, together with all the well known results about ESQPTs, suggets that the main requirement for the occurrence of an ESQPT is neither having a large number of particles behaving in a collective way, nor a QPT in the GS that propagates to higher energies, but the fact that the quantum system can be faithfully described by semiclassical

approximation with a finite number of degrees of freedom and a bifurcation in the classical phase space.

Moreover, our study in the TSEGM suggests that the ESQPTs are not just quantum manifestations of a classical phenomenon, but they also preserve some quantum properties. The most important one is the possibility of breaking certain discrete symmetries. For the TSEGM, the critical energy separates a region of broken parity symmetry, from another region of broken time-reversal symmetry. This feature constitutes a generalization of previous results showing that crossing an ESQPT comprises the appearance of degenerate parity doublets [18], which imply important dynamical consequences like the ones discussed in [19].

The paper is organized as follows. In Sec. II we introduce the two-spin elliptic Gaudin model and prove that it is always integrable by a second independent integral of motion. In Sec. III we study two discrete symmetries of the model: parity and time reversal. In Sec. IV we study the ESQPTs both analytically and numerically. Finally, in Sec. V we summarize our conclusions.

II. INTEGRABILITY OF THE TWO-SPIN GAUDIN MODEL

The elliptic Gaudin model was proposed by Gaudin [20] as a particular family of integrable spin Hamiltonians with a fully anisotropic spin-spin interaction. The N commuting Gaudin integrals of motion for a system of N arbitrary spins S_i^α, with $\alpha = x,y,z$ and $i = 1,\ldots,N$ are

$$R_i = \sum_{\substack{j=1\\(j\neq i)}}^{N} J_{ij}^x S_i^x S_j^x + J_{ij}^y S_i^y S_j^y + J_{ij}^z S_i^z S_j^z. \tag{1}$$

In order to fulfill the integrability conditions $[R_i,R_j] = 0$, the matrices J^α must satisfy the Gaudin conditions

$$J_{ij}^\alpha J_{jk}^\gamma + J_{ji}^\beta J_{ik}^\gamma + J_{ik}^\alpha J_{kj}^\beta = 0.$$

The coefficients J_{ij}^α in (1) can be expressed (Ref. [25]) by means of the doubly periodic elliptic Jacobi functions of modulus k, $\mathrm{sn}(z,k)$, $\mathrm{cn}(z,k)$ and $\mathrm{dn}(z,k)$ (for brevity, in general, we will not explicitly write the modulus k), and a set of N arbitrary coefficients z_i as

$$\begin{aligned} J_{ij}^x &= \frac{1 + k\,\mathrm{sn}^2(z_i - z_j)}{\mathrm{sn}(z_i - z_j)},\\ J_{ij}^y &= \frac{1 - k\,\mathrm{sn}^2(z_i - z_j)}{\mathrm{sn}(z_i - z_j)},\\ J_{ij}^z &= \frac{\mathrm{cn}(z_i - z_j)\,\mathrm{dn}(z_i - z_j)}{\mathrm{sn}(z_i - z_j)}. \end{aligned} \tag{2}$$

However, there are only $N-1$ independent integrals of this kind, since the matrices J^α are antisymmetric and the sum $\sum_i^N R_i$ is zero. A general expression for the remaining independent integral of motion was found by Sklyanin and Takebe [26] in terms of Weierstrass's elliptic and ζ functions.

The exact solution of the integrable elliptic model for a system of N spins $1/2$ was obtained by means of the algebraic Bethe ansatz [26] and later generalized to N arbitrary spins [21].

Let us now consider the particular case of two arbitrary spins defining the TSEGM. Taking $N = 2$ in (1), the model Hamiltonian is the first Gaudin integral of motion R_1 (note that $R_2 = -R_1$),

$$H = J_{12}^x S_1^x S_2^x + J_{12}^y S_1^y S_2^y + J_{12}^z S_1^z S_2^z. \tag{3}$$

In order to demonstrate that the two-spin system is quantum integrable, we will construct an independent second integral of motion Q by algebraic means without introducing new special functions. Let us define a symmetric quadratic operator for two spins,

$$\begin{aligned} Q = {} & q_{11}^x \left(S_1^x\right)^2 + q_{11}^y \left(S_1^y\right)^2 + q_{11}^z \left(S_1^z\right)^2 + q_{22}^x \left(S_2^x\right)^2 + q_{22}^y \left(S_2^y\right)^2 \\ & + q_{22}^z \left(S_2^z\right)^2 + q_{12}^x S_1^x S_2^x + q_{12}^y S_1^y S_2^y + q_{12}^z S_1^z S_2^z. \end{aligned} \tag{4}$$

We want to determine the set of coefficients q_{ij} that satisfies the integrability condition $[H,Q] = 0$. After some algebraic manipulations we get

$$\begin{aligned} [H,Q] = {} & i \sum_{\alpha<\beta,\gamma} \left(J_{12}^\alpha q_{12}^\beta - J_{12}^\beta q_{12}^\alpha - 2J_{12}^\gamma q_{11}^\beta + 2J_{12}^\gamma q_{11}^\alpha\right) \\ & \times \epsilon_{\alpha\beta\gamma}\, S_1^\alpha S_1^\beta S_2^\gamma + i \sum_{\alpha<\beta,\gamma} \left(J_{12}^\alpha q_{12}^\beta - J_{12}^\beta q_{12}^\alpha \right. \\ & \left. - 2J_{12}^\gamma q_{22}^\beta + 2J_{12}^\gamma q_{22}^\alpha\right)\epsilon_{\alpha\beta\gamma}\, S_2^\alpha S_2^\beta S_1^\gamma \\ & + \sum_{\alpha<\beta,\gamma} \left(J_{12}^\alpha q_{12}^\beta - J_{12}^\beta q_{12}^\alpha - J_{12}^\gamma q_{11}^\beta + J_{12}^\gamma q_{11}^\alpha \right. \\ & \left. - J_{12}^\gamma q_{22}^\beta + J_{12}^\gamma q_{22}^\alpha\right) \times \epsilon_{\alpha\beta\gamma}^2\, S_1^\gamma S_2^\gamma, \end{aligned}$$

where $\alpha < \beta$ implies a lexicographic order ($x < y < z$).

In what follows, we skip the subindexes of J^α and write $J^\alpha = J_{12}^\alpha$. The condition $[H,Q] = 0$ leads to the system of equations ($\alpha \neq \beta \neq \gamma$)

$$J^\alpha q_{12}^\beta - J^\beta q_{12}^\alpha - 2\,J^\gamma \left(q_{11}^\beta - q_{11}^\alpha\right) = 0, \tag{5}$$

$$J^\alpha q_{12}^\beta - J^\beta q_{12}^\alpha - 2\,J^\gamma \left(q_{22}^\beta - q_{22}^\alpha\right) = 0, \tag{6}$$

$$J^\alpha q_{12}^\beta - J^\beta q_{12}^\alpha - J^\gamma q_{11}^\beta + J^\gamma q_{11}^\alpha - J^\gamma q_{22}^\beta + J^\gamma q_{22}^\alpha = 0. \tag{7}$$

From the first and second equations we get $(q_{11}^\beta - q_{11}^\alpha) = (q_{22}^\beta - q_{22}^\alpha)$, and therefore both equations are equivalent. The third equation is just the sum of (5) and (6) and can be neglected.

In order to search for nontrivial solutions we will assume, without lost of generality, that $q_{11}^\alpha = q_{22}^\alpha$ (all other possibilities would lead to trivial solutions), and study the set of equations (5). This is a linear homogeneous system of equations for the unknowns q_{ij} in terms of the arbitrary coefficients J^α. If we order the vector of unknowns as $\mathbf{b} = (q_{12}^x, q_{12}^y, q_{12}^z, q_{11}^x, q_{11}^y, q_{11}^z)$, the coefficient matrix of the system is

$$\mathbf{A} = \begin{pmatrix} -J^y & J^x & 0 & 2J^z & -2J^z & 0 \\ -J^z & 0 & J^x & 2J^y & 0 & -2J^y \\ J^y & -J^x & 0 & -2J^z & 2J^z & 0 \\ 0 & -J^z & J^y & 0 & 2J^x & -2J^x \\ J^z & 0 & -J^x & -2J^y & 0 & 2J^y \\ 0 & J^z & -J^y & 0 & -2J^x & 2J^x \end{pmatrix}.$$

This is a matrix of dimension 6 and rank 3. Therefore, the system (5) has three linear independent solutions. Two of them are trivial, and the third one defines the independent integral of motion Q,

$$
\begin{aligned}
q_{11}^{x} &= \frac{1}{3}(-2J^{x2} + J^{y2} + J^{z2}),\\
q_{11}^{y} &= \frac{1}{3}(J^{x2} - 2J^{y2} + J^{z2}),\\
q_{11}^{z} &= \frac{1}{3}(J^{x2} + J^{y2} - 2J^{z2}),\\
q_{12}^{x} &= \frac{2J^{y}J^{z}}{J^{x2}+J^{y2}+J^{z2}}(-2J^{x2} + J^{y2} + J^{z2}),\\
q_{12}^{y} &= \frac{2J^{x}J^{z}}{J^{x2}+J^{y2}+J^{z2}}(J^{x2} - 2J^{y2} + J^{z2}),\\
q_{12}^{z} &= \frac{2J^{x}J^{y}}{J^{x2}+J^{y2}+J^{z2}}(J^{x2} + J^{y2} - 2J^{z2}).
\end{aligned}
$$

This solution of the TSEGM exists for arbitrary values of J^{α} and the system is always integrable. Even though the coefficients J^{α} could be expressed in terms of elliptic function as in (2), for simplicity we continue using this parametrization. We will restrict ourselves to the parameter region $J_{12}^{x} > J_{12}^{y} > J_{12}^{z}$, since the other regions of the parameters space can be accessed by appropriate rotations in the spin space.

III. SYMMETRIES OF THE TWO-SPIN ELLIPTIC GAUDIN MODEL

The two-spin integrals of motion (3) and (4) break the su(2) symmetry associated with the conservation of the total spin S and the u(1) symmetry associated with the conservation of the z component of the total spin S^{z}. However, the model preserves two discrete Z_2 symmetries. One of these is associated with a π rotation of every spin around an arbitrary axis. Assuming z as the quantization axis, a rotation by an angle π around this axis is related to the parity operator $\Pi = \prod_{i=1}^{N} \exp[i\pi(S_i^{z} + s_i)]$ with eigenvalues $+1$ for positive parity and -1 for negative parity. The second discrete symmetry is the time reversal. Taking into account that the time-reversal operator Θ is antiunitary, it can be expressed as $\Theta = K \prod_{i=1}^{N} \exp(-i\pi S_i^{y})$, where K is the charge conjugation operator, $K S^{x} K^{\dagger} = S^{x}$, $K S^{y} K^{\dagger} = -S^{y}$, and $K S^{z} K^{\dagger} = S^{z}$.

In order to analyze the action of the parity and the time-reversal operators on an arbitrary state $|\psi\rangle$ of the two-spin system, we will expand it in the uncoupled basis of S_i^{z} eigenstates $|m_1,m_2\rangle$ as $|\psi\rangle = \sum_{m_1 m_2} C_{m_1 m_2}|m_1,m_2\rangle$. Applying these operators we get

$$
\Pi|\psi\rangle = \sum_{m_1,m_2} C_{m_1,m_2} e^{i\pi(s_1+m_1+s_2+m_2)}|m_1,m_2\rangle, \tag{8}
$$

$$
\Theta|\psi\rangle = \sum_{m_1,m_2} \eta(-1)^{s_1+s_2-m_1-m_2} C^{*}_{m_1,m_2}|-m_1,-m_2\rangle, \tag{9}
$$

where η is an arbitrary phase which does not depend on m_1 or m_2. From these expressions it is straightforward to obtain the action of the commutator,

$$
\begin{aligned}
[\Theta,\Pi]|\psi\rangle = &-2i\eta \sum_{m_1,m_2} C^{*}_{m_1,m_2}(-1)^{s_1+s_2-m_1-m_2}\\
&\times e^{-i\pi(m_1+m_2)} \sin[\pi(s_1+s_2)]|-m_1,-m_2\rangle.
\end{aligned} \tag{10}
$$

Hence, if the total spin is integer we get $[\Theta,\Pi] = 0$, whereas if the total spin is half integer $[\Theta,\Pi] \neq 0$. As a consequence, every eigenstate of H and Q can be labeled (simultaneously) by Π and Θ for integer total spin, and by either Π or Θ for a half-integer total spin.

The fact that Π and Θ do not commute for half-integer total spin systems entails a very significant consequence for the structure of the corresponding spectra. Let us consider a state with positive parity defined as

$$
|\Pi_{+}\rangle = \sum_{m_1 m_2}^{+} C_{m_1 m_2}|m_1,m_2\rangle, \tag{11}
$$

where the superindex $+$ indicates that the sum is restricted over the set of m_1 and m_2 such that $s_1 + s_2 + m_1 + m_2$ is even; thus the phases appearing in Eq. (8) are always equal to 1. Now, if we act with the time-reversal operator (9) on $|\Pi_{+}\rangle$, we obtain

$$
\Theta|\Pi_{+}\rangle = \sum_{m_1,m_2}^{+} \eta(-1)^{s_1+s_2-m_1-m_2} C^{*}_{m_1,m_2}|-m_1,-m_2\rangle. \tag{12}
$$

Let us concentrate in the parity of the resulting state, computing $\Pi\Theta|\Pi_{+}\rangle$. For integer total spin, $s_1 + s_2 + m_1 + m_2$ and $s_1 + s_2 - m_1 - m_2$ are both even (or odd). The resulting phase in Eq. (8) is $+1$ in this case, consequently $\Pi\Theta|\Pi_{+}\rangle = \Theta|\Pi_{+}\rangle$ and the time-reversal operator does not change the parity of the state. This result comes from the fact that $[\Theta,\Pi] = 0$ for total spin integer. Analogously, for a state of negative parity we also obtain a state of negative parity $\Pi\Theta|\Pi_{-}\rangle = -\Theta|\Pi_{-}\rangle$. On the other hand, for systems with half-integer total spin, whenever $s_1 + s_2 + m_1 + m_2$ is even, $s_1 + s_2 - m_1 - m_2$ is odd and vice versa. Hence, the resulting phase in Eq. (8) is -1, consequently $\Pi\Theta|\Pi_{+}\rangle = -\Theta|\Pi_{+}\rangle$ and the time-reversal operator changes the parity of the state. Similarly, for a state of negative parity we obtain a state of positive parity $\Pi\Theta|\Pi_{-}\rangle = \Theta|\Pi_{-}\rangle$. As a consequence, for half-integer spin systems the eigenstates of Θ [i.e., $|\Theta_{+}\rangle$or$|\Theta_{-}\rangle$] are linear combinations of eigenstates of Π and vice versa,

$$
|\Theta_{\pm}\rangle = \frac{1}{\sqrt{2}}[|\Pi_{+}\rangle \pm |\Pi_{-}\rangle]. \tag{13}
$$

As we have already established above, there are two options to label the eigenstates of H and Q for a half-integer spin system. For instance, by means of the quantum numbers of H and Π (energy and parity),

$$
H|E^{\Pi}_{n,\pm}\rangle = E^{\Pi}_{n,\pm}|E^{\Pi}_{i,\pm}\rangle, \quad \Pi|E^{\Pi}_{n,\pm}\rangle = \pm|E^{\Pi}_{n,\pm}\rangle. \tag{14}
$$

However, we can also choose H and Θ, obtaining two different labels for the eigenstates,

$$
H|E^{\Theta}_{n,\pm}\rangle = E^{\Theta}_{n,\pm}|E^{\Theta}_{n,\pm}\rangle, \quad \Theta|E^{\Theta}_{n,\pm}\rangle = \pm|E^{\Theta}_{n,\pm}\rangle. \tag{15}
$$

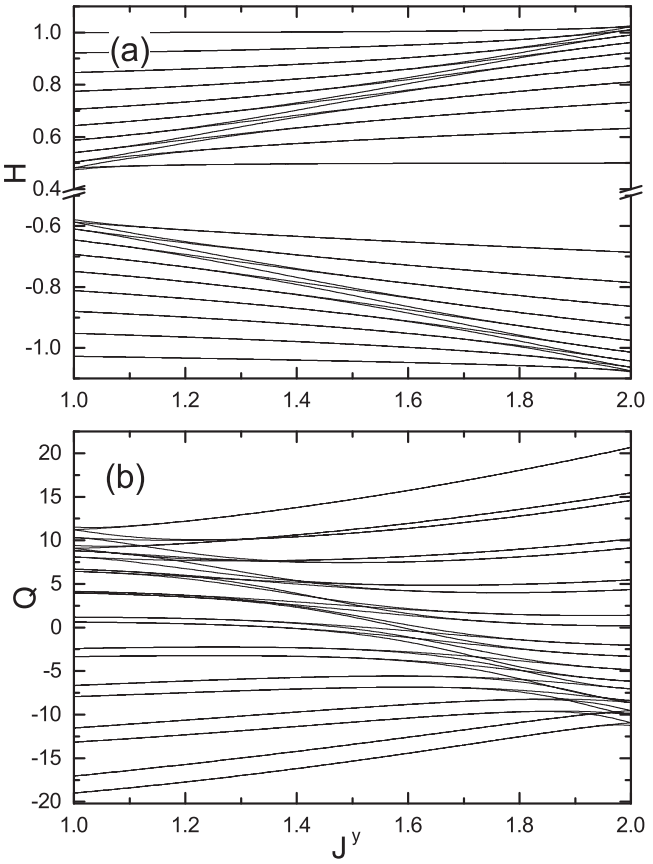

FIG. 1. Spectra of the two integrals of motion for $s_1 = 19/2$, $s_2 = 1/2$, $J^x = 2$, and $J^z = 1$ as a function J^y in the range $1 \leqslant J^y \leqslant 2$. H is shown in panel (a) and Q in panel (b).

Taking into account (13), we can write

$$H|E^{\Theta}_{n,\pm}\rangle = \frac{1}{\sqrt{2}} H[|E^{\Pi}_{n,+}\rangle \pm |E^{\Pi}_{n,-}\rangle] = \frac{1}{\sqrt{2}}[E^{\Pi}_{n,+}|E^{\Pi}_{n,+}\rangle \pm E^{\Pi}_{n,-}|E^{\Pi}_{n,-}\rangle]. \quad (16)$$

Since $|E^{\Theta}_{n,\pm}\rangle$ is an eigenstate of H, we conclude that $E^{\Pi}_{n,+} = E^{\Pi}_{n,-}$. Therefore, all energy levels are degenerate in pairs for half-integer spin systems. This is a manifestation of the Kramer's degeneracy [27].

For integer spin systems, the eigenstates of H and Q have good parity and time-reversal quantum numbers, but no exact degeneracies in the spectrum. Nonetheless, in the limit $J^y = J^x$ both integrals commute with the total z component $S^z_1 + S^z_2$, and in the limit $J^y = J^z$ both integrals commute with the total x component $S^x_1 + S^x_2$. Due to these extra symmetries the spectrum in both cases is double degenerate.

As an example we show in Fig. 1 the spectra of the two integrals of motion H (3) and Q (4) for a system with $s_1 = 19/2$, $s_2 = 1/2$, $J^x = 2$, and $J^z = 1$, as a function of J^y. The eigenstates of the system are a mixture of states with integer total spins $s = 9$ and 10. As seen in the figure, the spectrum of H is divided in two bands. In each of the bands, as well as in the spectrum of Q, we observe an accumulation of energy levels the constitutes a precursor of an ESQPT. In the lower band of H and in Q, this accumulation moves from the upper part of the spectrum to the lower part, reaching the ground state for $J^y = J^x = 2$. At this limit, both integrals of motion commute with the third component of the total spin S^z. Beyond this limit ($J^y > J^x$) one can always perform a rotation in π around the z axis such that $S^y \to -S^x$ and $S^x \to S^y$, which amounts to interchange J^y with J^x in H and Q. Therefore, the model is in the same phase at both sides of the limit $J^y = J^x = 2$.

IV. EXCITED-STATE QUANTUM PHASE TRANSITIONS

In this section we study first the TSEGM (3) in the semiclassical approximation ($s_1 \to \infty$) and then with exact diagonalizations for large values of s_1.

A. Semiclassical approximation

The analog of the thermodynamic limit is obtained when the large spin $s_1 \to \infty$, and the small spin s_2 remains finite. In this limit, the large spin s_1 can be described classically as

$$\vec{S}_1 = s_1(\sin\theta\cos\phi, \sin\theta\sin\phi, \cos\theta). \quad (17)$$

Inserting in the Hamiltonian (3), it is approximated as

$$\frac{H_{\rm class}}{s_1} = J^x_{12}\sin\theta\cos\phi S^x_2 + J^y_{12}\sin\theta\sin\phi S^y_2 + J^z_{12}\cos\theta S^z_2. \quad (18)$$

In the basis $|s_2 m_2\rangle$ this is a tridiagonal matrix of dimension $n = 2s_2 + 1$ that reads

$$\begin{pmatrix} -s_2 J^z_{12}\cos\theta & C_1\left(J^x_{12}\cos\phi + iJ^y_{12}\sin\phi\right)\sin\theta & 0 & \dots & 0 \\ C_1\left(J^x_{12}\cos\phi - iJ^y_{12}\sin\phi\right)\sin\theta & -(s_2-1)J^z_{12}\cos\theta & C_2\left(J^x_{12}\cos\phi + iJ^y_{12}\sin\phi\right)\sin\theta & \dots & 0 \\ 0 & C_2\left(J^x_{12}\cos\phi - iJ^y_{12}\sin\phi\right)\sin\theta & -(s_2-2)J^z_{12}\cos\theta & \dots & 0 \\ \vdots & \vdots & \vdots & \ddots & \vdots \\ 0 & 0 & \dots & C_{n-1}\left(J^x_{12}\cos\phi - iJ^y_{12}\sin\phi\right)\sin\theta & s_2 J^z_{12}\cos\theta \end{pmatrix} \quad (19)$$

with $C_k = \frac{1}{2}\sqrt{s_2(s_2+1) - (k-s_2-1)(k-s_2)}$.

For a system with a large single spin, like the LMG model, the same classical approximation is enough to obtain the critical coupling constant for the QPT [28], and the critical energy of the ESQPT, together with the smooth behavior of the physical observables at both sides of the transitions [7]. For our two-spin model, a similar picture can be obtained by diagonalizing (19). The corresponding eigenvalues are

obtained from the recurrence formula for the determinant of a tridiagonal matrix with a subsequent factorization of the characteristic polynomial [29]. For a half-integer spin s_2, the characteristic polynomial is

$$P(\lambda)=\frac{1}{4^{(2s_2+1)/2}}\prod_{k=1}^{(2s_2+1)/2}\left\{4\lambda^2-(2k-1)^2\cos^2\theta\left(J_{12}^z\right)^2-(2k-1)^2\sin^2\theta\left[\left(J_{12}^x\right)^2\cos^2\phi+\left(J_{12}^y\right)^2\sin^2\phi\right]\right\}, \tag{20}$$

with roots providing the eigenvalues of Eq. (19),

$$\lambda_k(\theta,\phi)=\pm\frac{2k-1}{2}\sqrt{\left(J_{12}^z\right)^2\cos^2\theta+\left[\left(J_{12}^x\right)^2\cos^2\phi+\left(J_{12}^y\right)^2\sin^2\phi\right]\sin^2\theta}, \tag{21}$$

for $k=1,2,\ldots,\frac{2s_2+1}{2}$.

For integer spin systems, the characteristic polynomial is

$$P(\lambda)=\lambda\prod_{k=1}^{s_2}\left\{\lambda^2-k^2\cos^2\theta\left(J_{12}^z\right)^2-k^2\sin^2\theta\left[\left(J_{12}^x\right)^2\cos^2\phi+\left(J_{12}^y\right)^2\sin^2\phi\right]\right\}, \tag{22}$$

with roots

$$\lambda_k(\theta,\phi)=\pm k\sqrt{\left(J_{12}^z\right)^2\cos^2\theta+\left[\left(J_{12}^x\right)^2\cos^2\phi+\left(J_{12}^y\right)^2\sin^2\phi\right]\sin^2\theta}, \tag{23}$$

for $k=1,2,\ldots,s_2$, together with $\lambda=0$.

These results can be understood considering that each eigenvalue $\lambda_k(\theta,\phi)$ is an energy band, comprising a subset of eigenvalues of the quantum system. The complete spectrum consists of the union of all these energy bands. This picture is specially revealing if the bands do not overlap. Then, each energy surface $\lambda_k(\theta,\phi)$ describes a different part of the spectrum, and hence the analysis of its singular points suffices to determine both the edges of the band and the critical energy of the ESQPT. On the contrary, if two or more bands overlap, a mixture of different energy surfaces is required to properly describe the spectrum. As a consequence the simple phenomenology arising from nonoverlapping bands becomes blurred. As we shall see below, this fact also implies that ESQPTs are progressively ruled out as the number of overlapping bands increases. Therefore, it is useful to determine the limits of the different bands, and to derive under which conditions all of them are well separated. From the general analysis that follows we have to exclude the particular cases $s_2=1/2$ and $s_2=1$ for which there is no overlap between bands for any value of the coupling constants. A straightforward calculation shows that the upper and lower limits of each band are

$$\lambda_k(\pi/2,0)=\lambda_k(\pi/2,\pi)=\pm\alpha_k J_{12}^x, \tag{24}$$

$$\lambda_k(0,\phi)=\lambda_k(\pi,\phi)=\pm\alpha_k J_{12}^z, \tag{25}$$

where $\alpha_k=(2k-1)/2$ if s_2 is a half integer, and $\alpha_k=k$, if s_2 is an integer. Note that in both cases, $\alpha_k=-s_2,-s_2+1,\ldots,s_2$. Hence, if

$$\alpha_k J_{12}^x<\alpha_{k+1}J_{12}^z, \tag{26}$$

all bands are separated, and therefore their classical structure gives a good approximation for the behavior of the TSEGM (3). As the widest bands are the ones at the edges of the spectrum, the most restrictive condition is

$$J_{12}^x<\frac{s_2}{s_2-1}J_{12}^z, \tag{27}$$

provided that $s_2>1$. Taking into account that we restrict ourselves to the parameter region $J_{12}^x>J_{12}^y>J_{12}^z$, we obtain the following condition:

$$\frac{s_2}{s_2-1}J_{12}^z>J_{12}^x>J_{12}^y>J_{12}^z, \tag{28}$$

for not having overlaps between the different bands in the spectrum. If this last condition is fulfilled, the semiclassical analysis provides a good description of the physics inside each band, including the critical points of the corresponding ESQPTs.

As the functional form of every energy band $E/s_1=\lambda_k(\theta,\phi)$ is the same, we can obtain valuable information just by drawing a contour plot of this function for a representative case. In Fig. 2, we show a contour plot for the first negative root $k=1$, with $J_{12}^x=3$, $J_{12}^y=2$, and $J_{12}^z=1$ and a half integer s_2. We remark the following features: (a) for $E/s_1<-1$, each curve of constant energy is split in two different regions: one centered at $(\theta,\phi)=(\pi/2,0)$, and the other centered at $(\theta,\phi)=(\pi/2,\pi)$; (b) for $E/s_1>-1$, each curve of constant energy is split again in two different regions, one with $\theta<\pi/2$, and the other with $\theta>\pi/2$, and both covering the whole range $0\leqslant\phi<2\pi$; (c) the separatrix at $E/s_1=-1$ is a nonanalytic curve, which crosses itself at $(\theta,\phi)=(\pi/2,\pi/2)$ and $(\theta,\phi)=(\pi/2,3\pi/2)$. This picture coincides with Eqs. (24) and (25), determining the upper and the lower bounds of every band. Furthermore, the nonanalytic points of the separatrix at $E/s_1=-1$ correspond to the saddle points of the surface $\lambda_k(\theta,\phi)$,

$$\lambda_k(\pi/2,\pi/2)=\lambda_k(\pi/2,3\pi/2)=\pm\alpha_k J_{12}^y. \tag{29}$$

From a physical point of view, these features entail a number of relevant consequences. Let us suppose that the system evolves from a certain initial condition, with a specific value

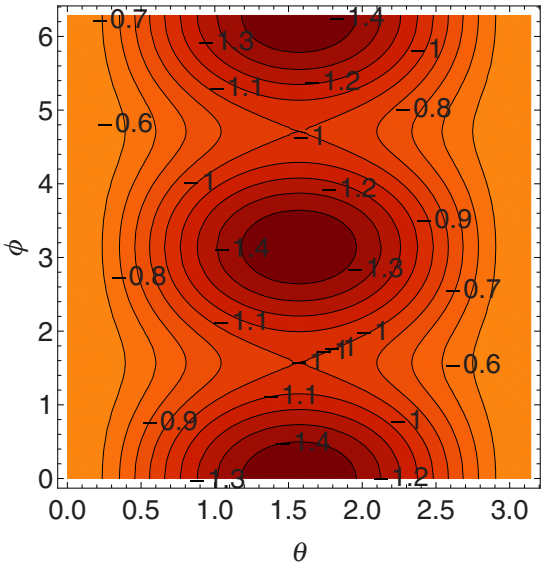

FIG. 2. Contour plot of $\lambda_1(\theta,\phi)$, $k=1$, $J^x_{12}=3$, $J^y_{12}=2$, and $J^z_{12}=1$. Darker (red online) regions correspond to the lower energy values; lighter regions (orange online) to the upper ones.

of the energy E/s_1. The corresponding classical trajectory covers the whole part of the constant energy curve in which the initial condition lies on. Therefore, we can consider that the time-average expectation values of the characteristic observables coincide with the geometric averages over those curves,

$$\langle \vec{S}_1 \rangle = s_1(\langle \sin\theta\cos\phi\rangle, \langle \sin\theta\sin\phi\rangle, \langle\cos\theta\rangle). \tag{30}$$

Hence, if $E/s_1 < -1$, $\langle S^y_1\rangle = \langle S^z_1\rangle = 0$ for any initial condition, and $\langle S^x_1\rangle \neq 0$, being positive if the initial condition is around $\phi = 0$, and negative if it is around $\phi = \pi$. On the contrary, if $E/s_1 > -1$, $\langle S^x_1\rangle = \langle S^y_1\rangle = 0$, and $\langle S^z_1\rangle \neq 0$, being positive if the initial condition is around $0 \leqslant \theta < \pi/2$, and negative if it is around $\pi/2 \leqslant \theta < \pi$. Translated into quantum language, and taking into account the definitions of the parity Π and the time-reversal Θ operators, this means that the parity symmetry can be broken if $E/s_1 < -1$, due to $\langle S^x_1\rangle \neq 0$, and, on the contrary, the time-reversal symmetry can be broken if $E/s_1 > -1$, due to $\langle S^z_1\rangle \neq 0$.

In other collective systems, a similar change of the symmetry-breaking behavior at a certain critical energy E_c is a signature of an ESQPT. For example, in the LMG model the parity symmetry can only be broken below the critical energy ($E < E_c$) implying that $\langle S^x\rangle \neq 0$. Also, the classical separatrix between these two regions is a nonanalytic curve, which crosses itself at the saddle point of the energy surface $H(p,q)$. Therefore, all the results shown in this section suggest that every energy band of the TSEGM (3), provided that the condition (28) is fulfilled, has en ESQPT at the critical energy given in Eq. (29). As a consequence, we can conclude that the energies

$$E_{c,k} = \pm\alpha_k J^y_{12} \tag{31}$$

are the critical energies of the ESQPT within each band.

On the other hand, there are no signatures of equivalent critical phenomena in the GS energy of the system or in each of the band heads. Contrary to what has been observed in all the collective models having ESQPTs, this phase transition does not follow from ground state QPT which propagates to excited states.

Upon inspection of Eqs. (24), (25), and (29), the saddle point signaling the ESQPT collapses with the lower or the upper states of the bands for $J^y_{12} \to J^x_{12}$ or $J^y_{12} \to J^z_{12}$, as it can also be seen in the example displayed in Fig. 1. Crossing these singular points is equivalent to rotating the spins $S^y \to S^x$ or $S^y \to S^z$, which does not alter the structure of the energy bands.

B. Exact diagonalization of the quantum system

The semiclassical description of the previous section can be tested against the exact numerical diagonalization of Eq. (3) for large systems. In Fig. 3 we show the density of states of a system with $s_1 = 9999/2$ and $s_2 = 9/2$, for energies lower than zero (the total spectrum is approximately symmetric around $E = 0$). In panel (a), we display a case with $J^x_{12} = 1.2$, $J^y_{12} = 1.1$, and $J^z_{12} = 1.0$. These values fulfill the condition given in Eq. (28), which in this case is $J^x_{12} < (9/7)J^z_{12} \sim 1.28J^z_{12}$. As a consequence, all the bands are well separated and all of them show a cusp singularity in their centers. Panel (b) displays a case with $J^x_{12} = 1.3$, $J^y_{12} = 1.15$, and $J^z_{12} = 1.0$. For these couplings the condition (28) is not fulfilled for the first band, but it it is fulfilled for the other bands [the second and third bands are separated if $J^x_{12} < (7/5)J^z_{12} = 1.4J^z_{12}$]. Despite of this fact, we still see cusp singularities in the first two bands. In addition, there is a jump in the density of states signaling the energy region at which these two bands overlap. The cusp singularity is a remanent of the ESQPT, which is still present because the overlap between the first and the second bands is not too large. On the contrary, the jump is not an ESQPT despite its nonanalytic behavior. It arises as a consequence of the overlap between the two bands. The point at which the

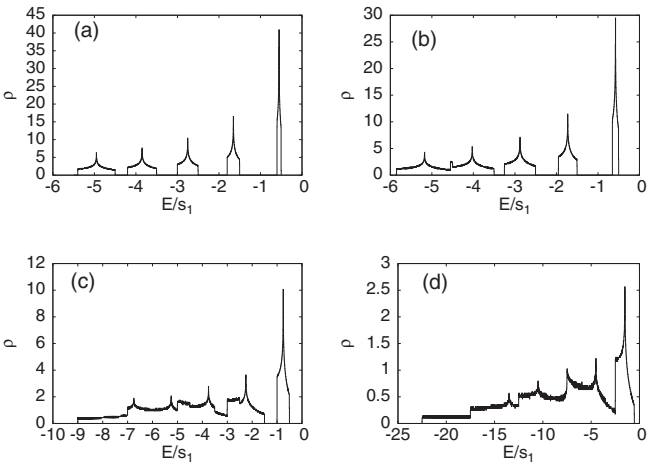

FIG. 3. Density of states for $s_1 = 9999/2$, and $s_2 = 9/2$. Panel (a), $J^x_{12} = 1.2$, $J^y_{12} = 1.1$, and $J^z_{12} = 1.0$. Panel (b), $J^x_{12} = 1.3$, $J^y_{12} = 1.15$, and $J^z_{12} = 1.0$. Panel (c), $J^x_{12} = 2.0$, $J^y_{12} = 1.5$, and $J^z_{12} = 1.0$. Panel (d), $J^x_{12} = 5.0$, $J^y_{12} = 3.0$, and $J^z_{12} = 1.0$.

jump takes place is the one at which the second band starts, and the abrupt increase of the density of states reflects the fact that a new set of energy levels appears at this energy.

The remaining three bands behave in a similar way as in panel (a), because they do fulfill the condition (28). The density of states in panel (c) shows no clear traces of cusp singularities up to the fifth band due to the mixture between the lower bands. Here the condition (28) only holds for the fifth band, and this is the unique band which is clearly separated from the rest, displaying a neat signature of an ESQPT. Finally, panel (d) presents results for a case where none of the bands fulfill Eq. (28). As a consequence the mixture of bands destroys most of the signatures of the ESQPTs in the density of states, the fifth band being the only one which retains a precursor of the cusp singularity.

The results shown in Fig. 3 provide a quantitative test of the semiclassical predictions. Eqs. (24), (25), and (29) establish the upper and lower bounds of every band and the critical energy of the ESQPT, respectively. For the first band in panel (a) these values are as follows: lower bound, $E_-/s_1 = -5.4$; upper bound $E_+/s_1 = -4.5$, and critical energy, $E_c/s_1 = -4.95$. The numerical results obtained by exact diagonalizations are very close to these values (see, for example, Fig. 4), $E_-/s_1 = -5.401$, $E_+/s_1 = -4.501$, $E_c/s_1, -4.951$. The small discrepancies can be attributed to finite-size corrections to the semiclassical approximation. If the values of J^x_{12}, J^y_{12}, and J^z_{12} are similar, we can investigate these finite-size corrections by

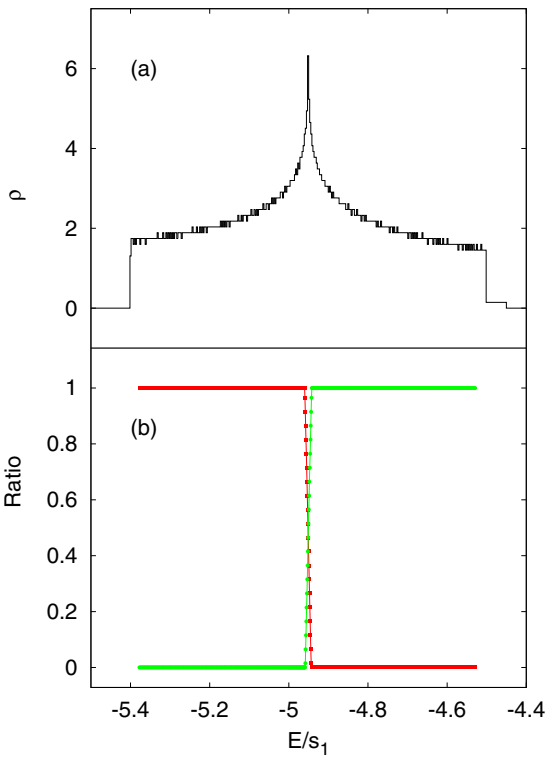

FIG. 4. Density of states and ratio of doublets for $s_1 = 9999/2$, $s_2 = 9/2$, $J^x_{12} = 1.2$, $J^y_{12} = 1.1$, and $J^z_{12} = 1.0$. Panel (a) shows the density of states of the first band. For the same band, panel (b) displays the ratio of doublets. Squares (red online) show parity doublets, while circles (green online) time-reversal doublets.

means of perturbation theory. The Hamiltonian can be written as $H = H_0 + V$, with

$$\begin{aligned} H_0 &= \frac{J^x_{12} + J^z_{12}}{2}\vec{S}_1 \cdot \vec{S}_2, \\ V &= \frac{J^x_{12} - J^z_{12}}{2}S^x_1 S^x_2 + \frac{2J^y_{12} - J^x_{12} - J^z_{12}}{2}S^y_1 S^y_2 \\ &\quad + \frac{J^z_{12} - J^x_{12}}{2}S^z_1 S^z_2. \end{aligned} \tag{32}$$

The spectrum of H_0 has a simple analytical solution,

$$\begin{aligned} H_0|sm\rangle = \frac{J^x_{12} + J^z_{12}}{4}&[s(s+1) \\ &- s_1(s_1+1) - s_2(s_2+1)]|sm\rangle, \end{aligned} \tag{33}$$

where s and m represent the total spin and its third component, respectively, and $s_1 - s_2 \leqslant s \leqslant s_1 + s_2$.

These unperturbed energy levels can be identified with the center of the bands, provided that the perturbation V is small enough. If we consider the index $n = -s_2, -s_2+1, \ldots, s_2$, the eigenvalues of (33) are

$$\begin{aligned} E_{0,n} &= \frac{J^x_{12} + J^z_{12}}{4}[(s_1+n)(s_1+n+1) \\ &\quad -s_1(s_1+1) - s_2(s_2+1)] \\ &= \frac{ns_1\left(J^x_{12} + J^z_{12}\right)}{2}\left[1 + \frac{n^2 + n - s_2^2 - s_2}{2ns_1}\right]. \end{aligned} \tag{34}$$

Since Eqs. (24) and (25) represent the upper and lower limit of each band, we take the average to define the centroid of the band, $\overline{E_{0,n}}/s_1 = \pm\alpha_n \frac{J^z_{12}+J^x_{12}}{2}$. Comparing with the unperturbated quantum centroids (34) we see that they already contain a finite-size correction of order $O(1/s_1)$ For the first band in Fig. 3(a), this correction is $\Delta E \sim 10^{-3}$, in excellent agreement with the exact results.

Besides this cusp singularity in the density of states, another signature of the ESQPT is the change from double-degenerate energy levels to nondegenerate energy levels, as is the case in the LMG or the Dicke models. More general models in higher dimensions display a degeneracy of different angular momentum states at one side of the critical energy, which is broken on the other side [3]. This fact is closely related to the different possibilities of symmetry breaking at both sides of the transition. In both the LMG and the Dicke models, the parity symmetry can only be broken below the critical energy. Within this region, the spectrum has parity doublets, any combination of such eigenstates is also an eigenstate, and thus it is possible to find steady-state states in which the parity symmetry is broken. On the contrary, if the energy is above the critical, there is no possibility of such a symmetry breaking. The picture of the TSEGM differs from the other models due to the existence of two Z_2 symmetries, parity Π, and time reversal Θ. However, as it has been discussed in the previous section, ESQPT could also separate two regions with different broken symmetries. In this case, the classical approximation states that below the critical energy only the parity symmetry can be broken, while above the critical energy only time-reversal symmetry can be broken. We then expect parity doublets below the critical energy, and time-reversal doublets above it.

Figure 4 shows the density of states and the ratio of doublets of the lowest band for the case of $s_1 = 9999/2$, $s_2 = 9/2$, $J_{12}^x = 1.2$, $J_{12}^y = 1.1$, and $J_{12}^z = 1.0$. (Note that the total spin of the system is an integer.) The number of doublets has been obtained in the following way: (i) We choose a window of $\Delta = 200$ energy levels; (ii) inside this window, we calculate the relative distance $d(E_{n+1}, E_n)$ between each pair of near neighbor levels; (iii) if this distance $d(E_{n+1}, E_n)$ is smaller than 10^{-8}, we consider that the pair constitutes a doublet (different quantitative results are obtained with other bounds, but the qualitative shape of the ratio persists); (iv) finally, we determine the nature of the doublets by studying the parity and time-reversal quantum number of each level in the pair. If the two energy levels have the same time-reversal quantum number and opposite parity quantum numbers they form a parity doublet. If they have the same parity quantum number and opposite time-reversal quantum numbers they form a time-reversal doublet. As it can be seen in Fig. 4, the numerical results plainly confirm the previous description of the ESQPT. The critical energy is characterized by cusp singularity in the density of states, and the nature of the doublets changes abruptly from parity to time reversal.

The behavior of the doublets is more complex if the bands overlap. In Fig. 5 we plot the density of states and the ratio of doublets for $J_{12}^x = 5.0$, $J_{12}^y = 3.0$, and $J_{12}^z = 1.0$. In this case all the bands are mixed. In the lower part of the spectrum all levels pair in parity doublets implying that the parity symmetry is broken. For higher energies the bands start to overlap reflecting a mixture of parity and time-reversal doublets.

Expectation values of certain observables can be useful to identify the critical energy of an ESQPT. Though they are not order parameters, they do show a nonanalytic behavior at the critical point. For the TSEGM, the choice of these observables is complicated because of the two Z_2 discrete symmetries and the presence of degeneracies. Every energy level E_n with well defined parity satisfies $\langle S^x \rangle_n = 0$. Analogously, for every energy level E_n with well defined time reversal $\langle S^z \rangle_n = 0$. Therefore, systems with total integer spin have $\langle S^x \rangle_n = \langle S^z \rangle_n = 0$ in the eigenbasis with good Π and Θ, while for systems with total half-integer spin we can choose an eigenbasis conserving either Π or Θ. Alternatively, and due to the degeneracies, it is possible to use an eigenbasis without well defined values of Π or Θ. For the case of integer total spin, we can select an eigenbasis for which $\langle S^x \rangle_n \neq 0$ below the critical energy, and $\langle S^z \rangle_n \neq 0$ above the critical energy. For half-integer total spin systems, we can select an eigenbasis for which $\langle S^x \rangle_n \neq 0$ and $\langle S^z \rangle_n = 0$ for any doublet, or vice versa. In this regard, we choose the total spin S^2 and the square of the z component $(S^z)^2$, which are free of these ambiguities, as signatures of the ESQPT.

In Fig. 6 we plot $\langle S^2 \rangle_n$ and $\langle (S^z)^2 \rangle_n$ for the same parameters $(J_{12}^x, J_{12}^y, J_{12}^z)$ as in Fig. 3(a). The size of the large spin s_1 has been reduced to $s_1 = 999/2$ because the computation of observables is more demanding. Both observables show a clear nonanalytical dip at the critical energy of the ESQPT. However, none of them behave like an order parameter with a zero value in one phase and a finite value in the other. $\langle S^2 \rangle_n$ is almost

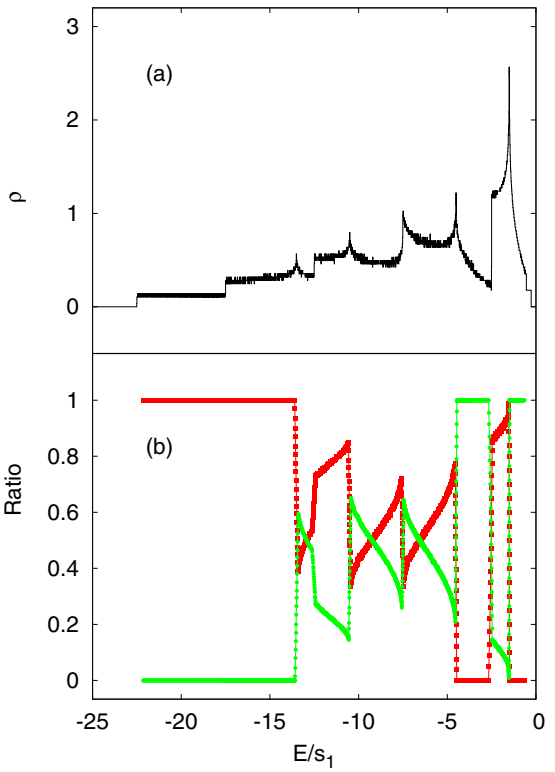

FIG. 5. Density of states and ratio of doublets for $s_1 = 9999/2$, $s_2 = 9/2$, $J_{12}^x = 5.0$, $J_{12}^y = 3.0$, and $J_{12}^z = 1.0$. Panel (a) shows the density of states of the first band. For the same band, panel (b) displays the ratio of doublets. Squares (red online) show parity doublets, while circles (green online) show time-reversal doublets.

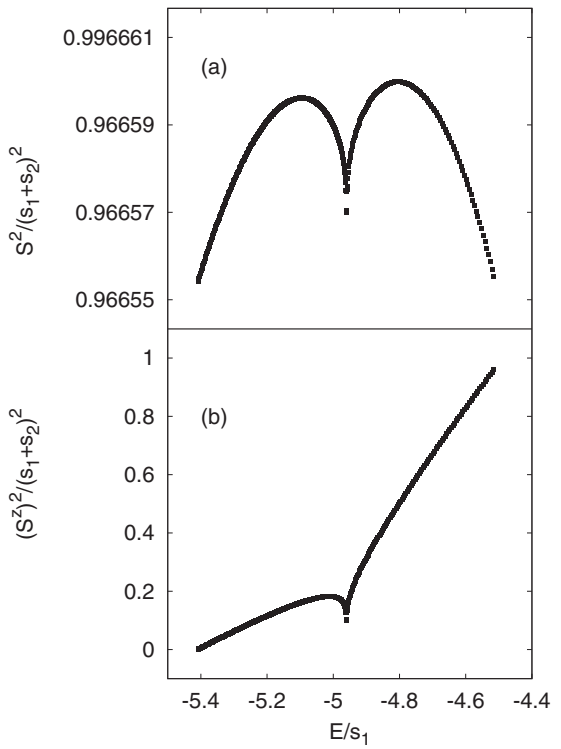

FIG. 6. Expectation values of S^2 and $(S^z)^2$, for the first band of a system with $s_1 = 999/2$, $s_2 = 9/2$, $J_{12}^x = 1.2$, $J_{12}^y = 1.1$, and $J_{12}^z = 1.0$. Panel (a) shows $\langle S^2 \rangle_n$; panel (b), $\langle (S^z)^2 \rangle_n$.

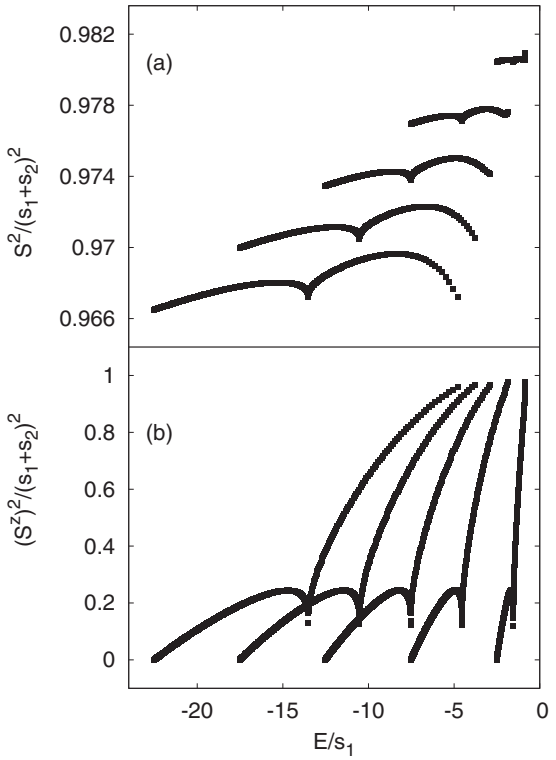

FIG. 7. Expectation values of S^2 and $(S^z)^2$, for a system with $s_1 = 999/2$, $s_2 = 9/2$, $J_{12}^x = 5.0$, $J_{12}^y = 3.0$, and $J_{12}^z = 1.0$. Panel (a) shows $\langle S^2\rangle_n$; panel (b), $\langle (S^z)^2\rangle_n$.

constant inside the band [notice the scale of panel (a)]. This fact can be understood from the perturbation approach of (32). The zero-order approximation for the energies $E_{0,n}$ establishes that each band is characterized by a different value of the total spin s. Applied to the case plotted in the figure, the result for $s(s+1)/(s_1+s_2)^2 = 0.9666$, which perfectly accounts for the numerics. The perturbation V from Eq. (32) slightly breaks the conservation of the total spin, $[H, S^2] \neq 0$, which holds for H_0.

Figure 7 shows the same observables of Fig. 6 for the parameters in panel (d) of Fig. 3. The overlap between the different bands implies that the expectation values $\langle S^2\rangle_n$ and $\langle (S^z)^2\rangle_n$ oscillate, depending on the band to which the level E_n belongs. Nevertheless, we can still see a residue of the critical points. It is also worthwhile to mention that the different bands, though overlapping, are still roughly characterized by a fixed value of s, which corresponds to $s(s+1)/(s_1+s_2)^2 = 0.9666,\ 0.9705,\ 0.9744, 0.9783$, and 0.9822 for the five bands plotted in the figure, which are pretty similar to the numerical results.

V. SUMMARY

We have shown that the two-spin Gaudin model is quantum integrable for arbitrary spins and arbitrary values of the coupling constants by finding a second integral of motion Q, which always fulfills $[H, Q] = 0$. The model has two discrete symmetries, parity Π and time reversal Θ. However, these two symmetries do not commute if the total spin of the system is half integer. As a consequence, the complete set of commuting operators can be either $\{H, Q, \Pi\}$ or $\{H, Q, \Theta\}$, and all the energy levels are double degenerated. On the contrary, $[\Pi, \Theta] = 0$ if the total spin is an integer, and therefore the complete set of commuting operators is $\{H, Q, \Pi, \Theta\}$.

If a small spin is coupled to a very large spin, the TSEGM has ESQPTs. For a finite large spin, numerical diagonalizations show finite-size precursors for such transitions, the critical behavior being reached when the size of the larger spin tends to infinity. If certain conditions of the coupling constants are fulfilled, the spectrum of the model is divided into independent bands, each one characterized by just one semiclassical degree of freedom. Each band displays an ESQPT, with a critical energy E_c which can be obtained from a semiclassical description. This critical energy splits the band into a region in which the parity symmetry is broken, from another region in which the time-reversal symmetry is broken. Moreover, the density of states and the expectation values of selected spin operators become singular at this energy value, showing a similar behavior as, for example, the Lipkin-Meshkov-Glick model. On the contrary, if the conditions required for having an ESQPT are not fulfilled, the different bands overlap and singularities are washed out.

In a different respect, this model constitutes an interesting example of a system in which ESQPTs take place without reaching a proper thermodynamical limit (neither the number of spin tends to infinity, nor does the size of all of them). Furthermore, contrary to what has been reported prior to this work in all other systems analyzed, the ESQPT exists *without* the corresponding QPT. These facts allows us to conclude that the main requirements for having ESQPTs are (i) the system has a proper semiclassical limit with a finite number of degrees of freedom, and (ii) the corresponding phase space undergoes a bifurcation. Moreover, we have also shown that ESQPTs in the TSEGM have a quantum origin due to the mechanism of abruptly changing from one discrete broken symmetry to another discrete broken symmetry when crossing the critical energy.

The TSEGM can be consider as an schematic model of the interaction of a central electron spin with the nuclear spins of a quantum dot in the limit in which the dot spins are reduced to a single collective spin. A typical number of nuclear spins in quantum dots is $\sim 10^4$–10^6 resulting in a very large collective spin. The strong anisotropies induced by the quadrupole coupling between the electron spin and the quantum dot, when it is comparable to the hyperfine interaction, could be modeled by our TSEGM Hamiltonian (3). The study of decoherence [8] and relaxation effects in these systems [30] could give clues about the presence of ESQPTs.

Extensions to systems with three or more spins can be employed to explore the properties of ESQPTs in systems with few semiclassical degrees of freedom. The existence of integrable limits, like the elliptic Gaudin model, could be useful to study the relation between this type of critical phenomenon and the emergence of quantum chaos.

ACKNOWLEDGMENTS

We acknowledge support from the Spanish Ministry of Economy and Competitiveness through Grants No. FIS2012-34479, No. FIS2012-35536, and from MINECO (Spain) and FEDER (Spain) Grant No. FIS2015-63770-P.

[1] P. Cejnar, M. Macek, S. Heinze, J. Jolie, and J. Dobes, J. Phys. A **39**, L515 (2006).
[2] P. Cejnar and P. Stránský, Phys. Rev. E **78**, 031130 (2008).
[3] M. A. Caprio, P. Cejnar, and F. Iachello, Ann. Phys. **323**, 1106 (2008).
[4] P. Stránský, M. Macek, and P. Cejnar, Ann. Phys. **345**, 73 (2014); P. Stránský, M. Macek, A. Leviatan, and P. Cejnar, *ibid.* **356**, 57 (2015).
[5] S. Sachdev, *Quantum Phase Transitions* (Cambridge University Press, Cambridge, UK, 2001); M. Vojta, Rep. Prog. Phys. **66**, 2069 (2003).
[6] W. D. Heiss and M. Müller, Phys. Rev. E **66**, 016217 (2002); F. Leyvraz and W. D. Heiss, Phys. Rev. Lett. **95**, 050402 (2005).
[7] P. Ribeiro, J. Vidal, and R. Mosseri, Phys. Rev. E **78**, 021106 (2008).
[8] A. Relaño, J. M. Arias, J. Dukelsky, J. E. García-Ramos, and P. Pérez-Fernández, Phys. Rev. A **78**, 060102(R) (2008); P. Pérez-Fernández, A. Relaño, J. M. Arias, J. Dukelsky, and J. E. García-Ramos, *ibid.* **80**, 032111 (2009); L. F. Santos, M. Távora, and F. Pérez-Bernal, *ibid.* **94**, 012113 (2016).
[9] P. Pérez-Fernández, A. Relaño, J. M. Arias, P. Cejnar, J. Dukelsky, and J. E. García-Ramos, Phys. Rev. E **83**, 046208 (2011); T. Brandes, *ibid.* **88**, 032133 (2013).
[10] J. M. Arias, J. Dukelsky, and J. E. García-Ramos, Phys. Rev. Lett. **91**, 162502 (2003); P. Cejnar, J. Jolie, and R. F. Casten, Rev. Mod. Phys. **82**, 2155 (2010).
[11] F. Pérez-Bernal and F. Iachello, Phys. Rev. A **77**, 032115 (2008); F. Pérez-Bernal and O. Álvarez-Bajo, *ibid.* **81**, 050101(R) (2010).
[12] A. Relaño, J. Dukelsky, P. Pérez-Fernández, and J. M. Arias, Phys. Rev. E **90**, 042139 (2014).
[13] V. M. Bastidas, P. Pérez-Fernández, M. Vogl, and T. Brandes, Phys. Rev. Lett. **112**, 140408 (2014).
[14] R. Puebla, M.-J. Hwang, and M. B. Plenio, Phys. Rev. A **94**, 023835 (2016).
[15] D. Larese and F. Iachello, J. Mol. Struct. **1006**, 611 (2011); D. Larese, F. Pŕez-Bernal, and F. Iachello, *ibid.* **1051**, 310 (2013); D. Larese, M. A. Caprio, F. Pérez-Bernal, and F. Iachello, J. Chem. Phys. **140**, 014304 (2014); N. F. Zobov, S. V. Shirin, O. L. Polyansky, J. Tennyson, P.-F. Coheur, P. F. Bernath, M. Carleer, and R. Colin, Chem. Phys. Lett. **414**, 193 (2006).
[16] B. Dietz, F. Iachello, M. Miski-Oglu, N. Pietralla, A. Richter, L. von Smekal, and J. Wambach, Phys. Rev. B **88**, 104101 (2013).
[17] L. Zhao, J. Jiang, T. Tang, M. Webb, and Y. Liu, Phys. Rev. A **89**, 023608 (2014).
[18] R. Puebla, A. Relaño, and J. Retamosa, Phys. Rev. A **87**, 023819 (2013); R. Puebla and A. Relaño, Europhys. Lett. **104**, 50007 (2013).
[19] R. Puebla and A. Relaño, Phys. Rev. E **92**, 012101 (2015).
[20] M. Gaudin, J. Phys. (Paris) **37**, 1087 (1976).
[21] C. Esebbag and J. Dukelsky, J. Phys. A **48**, 475303 (2015).
[22] K. Huang, *Statistical Mechanics* (Wiley, New York, 1987).
[23] M.-J. Hwang, R. Puebla, and M. B. Plenio, Phys. Rev. Lett. **115**, 180404 (2015); M.-J. Hwang and M. B. Plenio, *ibid.* **117**, 123602 (2016).
[24] J. M. Arias, J. E. García-Ramos, and J. Dukelsky, Phys. Rev. Lett. **93**, 212501 (2004); J. E. García-Ramos, P. Pérez-Fernández, J. M. Arias, and E. Freire, Phys. Rev. C **93**, 034336 (2016).
[25] H. Babujian, R. H. Poghossian, and A. Lima-Santos, Int. J. Mod. Phys. A **14**, 615 (1999).
[26] E. K. Sklyanin and T. Takebe, Phys. Lett. A **219**, 217 (1996).
[27] M. Lax, *Symmetry Principles in Solid State and Molecular Physics* (Wiley, New York, 1974).
[28] R. Botet, R. Jullien, and P. Pfeuty, Phys. Rev. Lett. **49**, 478 (1982).
[29] G. H. Golub and C. F. Van Loan, *Matrix Computations* (Johns Hopkins University Press, Baltimore, 1996).
[30] N. A. Sinitsyn, Y. Li, S. A. Crooker, A. Saxena, and D. L. Smith, Phys. Rev. Lett. **109**, 166605 (2012).